Genome-wide identification of the MADS-box gene family in *Avena sativa* and its role in photoperiod-insensitive oat

Jinsheng Nan [1], **Jianghong An** [1, 2], **Yan Yang** [1], **Guo-fen Zhao** [1], **Xiaohong Yang** [3], **Hui-Yan Liu** [1], **Bing Han** [Corresp. 1]

[1] Inner Mongolia Agricultural University, Key Lab of Germplasm Innovation and Utlization of Triticeae Crop at Universities of Inner Mongolia Autonomous Region, Inner Mongolia Agricultural University, Hohhot, Inner Mongolia, China

[2] Inner Mongolia Academy of Agriculture and Animal Husbandry Science, Hohhot, Inner Mongolia, China

[3] Zhangjiakou Academy of Agricultural Sciences, Zhangjiakou, HeBei Province, China

Corresponding Author: Bing Han
Email address: hb_nmg@163.com

Background. Traditional spring-summer sown oat is a typical long-day crop that cannot head under short-day conditions. The creation of photoperiod-insensitive oats overcomes this limitation. MADS-box genes are a class of transcription factors involved in plant flowering signal transduction regulation. Previous transcriptome studies have shown that MADS-box genes may be related to the oat photoperiod. **Methods.** Putative MADS-box genes were identified in the whole genome of oat. Bioinformatics methods were used to analyze their classification, conserved motifs, gene structure, evolution, chromosome localization, collinearity and *cis*-elements. Ten representative genes were further screened via qRT–PCR analysis under short days. **Results.** In total, sixteen *AsMADS* genes were identified and grouped into 9 subfamilies. The domains, conserved motifs and gene structures of all *AsMADS* genes were conserved. All members contained light-responsive elements. Using the photoperiod-insensitive oat MENGSIYAN4HAO (MSY4) and spring-summer sown oat HongQi2hao (HQ2) as materials, qRT–PCR analysis was used to analyze the *AsMADS* gene at different panicle differentiation stages under short-day conditions. Compared with HQ2, *AsMADS3*, *AsMADS8*, *AsMADS11*, *AsMADS13*, and *AsMADS16* were upregulated from the initial stage to the branch differentiation stage in MSY4, while *AsMADS12* was downregulated. qRT–PCR analysis was also performed on the whole panicle differentiation stages in MSY4 under short-day conditions, the result showed that the expression levels of *AsMADS9* and *AsMADS11* gradually decreased. Based on the subfamily to which these genes belong, the above results indicated that *AsMADS* genes, especially SVP, SQUA and Mα subfamily members, regulated panicle development in MSY4 by responding to short-days. This work provides a foundation for revealing the function of the *AsMADS* gene family in the oat photoperiod pathway.

1 **Genome-wide identification of the MADS-box gene family in *Avena sativa* and its**
2 **role in photoperiod-insensitive oat**

4 Jin-sheng Nan[1], Jiang-hong An[1, 2], Yan Yang[1], Guo-fen Zhao[1], Xiao-hong Yang[3], Hui-yan Liu[1],
5 Bing Han[1,*]
6
7 [1] Key Lab of Germplasm Innovation and Utlization of Triticeae Crop at Universities of Inner
8 Mongolia Autonomous Region, Inner Mongolia Agricultural University, Hohhot, 010018, China
9 [2] Inner Mongolia Academy of Agricultural & Animal Husbandry Sciences, Hohhot, 010031,
10 China
11 [3] Zhangjiakou Academy of Agricultural Sciences, Zhangjiakou, 075000, China
12
13 Corresponding Author:
14 Bing Han[1]
15 No. 306, Zhaowuda Road, Saihan District, Hohhot, Inner Mongolia, 010018, China.
16 Email address: hb_nmg@163.com (B. Han)

18
19
20
21
22 **Abstract**

23 **Background.** Traditional spring-summer sown oat is a typical long-day crop that cannot head
24 under short-day conditions. The creation of photoperiod-insensitive oats overcomes this
25 limitation. MADS-box genes are a class of transcription factors involved in plant flowering
26 signal transduction regulation. Previous transcriptome studies have shown that MADS-box genes
27 may be related to the oat photoperiod.
28 **Methods.** Putative MADS-box genes were identified in the whole genome of oat. Bioinformatics
29 methods were used to analyze their classification, conserved motifs, gene structure, evolution,
30 chromosome localization, collinearity and *cis*-elements. Ten representative genes were further
31 screened via qRT−PCR analysis under short days.
32 **Results.** In total, sixteen *AsMADS* genes were identified and grouped into 9 subfamilies. The
33 domains, conserved motifs and gene structures of all *AsMADS* genes were conserved. All
34 members contained light-responsive elements. Using the photoperiod-insensitive oat
35 MENGSIYAN4HAO (MSY4) and spring-summer sown oat HongQi2hao (HQ2) as materials,
36 qRT−PCR analysis was used to analyze the *AsMADS* gene at different panicle differentiation
37 stages under short-day conditions. Compared with HQ2, *AsMADS3*, *AsMADS8*, *AsMADS11*,
38 *AsMADS13*, and *AsMADS16* were upregulated from the initial stage to the branch differentiation
39 stage in MSY4, while *AsMADS12* was downregulated. qRT−PCR analysis was also performed
40 on the whole panicle differentiation stages in MSY4 under short-day conditions, the result

41 showed that the expression levels of *AsMADS9* and *AsMADS11* gradually decreased. Based on
42 the subfamily to which these genes belong, the above results indicated that *AsMADS* genes,
43 especially SVP, SQUA and Mα subfamily members, regulated panicle development in MSY4 by
44 responding to short-days. This work provides a foundation for revealing the function of the
45 *AsMADS* gene family in the oat photoperiod pathway.
46
47 **Keywords.** *Avena sativa* L; MADS-box gene family; Photoperiod; Short-day; Gene expression
48
49 **Introduction**
50 Among the cereal crops, oat (*Avena sativa* L.) is cultivated worldwide as a food and forage crop.
51 Traditional spring-summer sown oat is a long-day crop that cannot head without light in winter
52 in the Northern Hemisphere (Yang et al., 2018). This traditional oat generally requires at least 14
53 h of sunlight per day to head (An et al., 2018). This feature of oats limits the expansion of the oat
54 growing area. New photoperiod-insensitive germplasm was bred by "Interspecific Polymer
55 Crossing Methods" and could complete the entire growth period and set seeds in natural short-
56 day conditions in HaiNan, China (11 h light/13 h dark) (Yang et al., 2014). The creation of this
57 new oat germplasm overcame the previous limitations of photoperiod-sensitive oat. However,
58 the reason why photoperiod-insensitive oats can complete the growth period under short days has
59 not been elucidated. Transcriptome studies have been conducted previously on photoperiod-
60 insensitive materials and traditional oats, revealing that MADS genes may be related to the
61 photoperiod insensitivity of oat (An et al., 2020).
62 As transcriptional regulatory factors, MADS-box proteins play a key role in controlling the
63 signal transduction processes of plant flowering time, flower organ formation and meristem
64 specificity (Becker & Theissen 2003). Hundreds of MADS-box genes have been found in many
65 plants, such as Arabidopsis (Parenicová et al., 2003) maize (Zhao et al., 2011), rice (Arora et al.,
66 2007), and wheat (Susanne et al., 2020). There are two types of MADS-box genes in plants, type
67 I (SRF-like) and type II (MEF2-like, or MIKC type) (Smaczniak et al., 2012). Type I genes
68 usually contain only one or two exons, with one highly conserved SRF-like MADS domain, and
69 lack the K domain. Type II genes contain four conserved domain structures: the M domain
70 (MADS-box), I domain (Intervening), K domain (Keratin-Like) and C-terminal domain
71 (Henschel et al., 2002). Most of the MIKC-type MADS-box genes contain 6 introns and 7 exons,
72 called MIKC^C, while some contain 7 introns and 8 exons, called MIKC*. In Arabidopsis, the type
73 I MADS-box genes encode 3 types of proteins, including Mα, Mβ and Mγ types (Arora et al.,
74 2007). The MIKC^C proteins can be subdivided into 13 distinct subfamilies (AG, AGL6, AGL12,
75 AGL15, AGL17, DEF/GLO, BS, FLC, SEP/AGL2, SQUA, SVP, TM3/SOC1 and AP3) (Theien
76 2001). The MIKC* type can be divided into the P type and S type. The P-type MIKC* proteins
77 identified in Arabidopsis are AGL30, AGL65 and AGL94, and the S-type proteins are AGL66,
78 AGL67 and AGL104 (Michiel et al., 2012).
79 The ABCDE model is a classical genetic regulatory mechanism of flower organ development in
80 Arabidopsis (Theien 2001). AP1 is an A-type gene whose functions include recognition genes
81 that promote the formation of floral meristems and the development of sepals, petals and other

82   floral organs (Kempin et al., 1995). The AP1/SQUA homologous gene VRN1 in wheat is a
83   flowering activator and is regularly expressed in leaves under long- and short-day conditions.
84   VRN1 is located upstream of FT, upregulates FT expression and promotes flowering under long-
85   day conditions (Shimada et al., 2009). DEF/GLO is a B-class gene that controls the morphology
86   of the floral organs such as stamens and petals (Kai-Uwe et al., 2002). In Arabidopsis, the
87   formation of sepals, petals, stamens, carpels and ovules is related to the SEP gene, which forms a
88   MADS protein complex with A, B, C, and D proteins to work together in the morphogenesis of
89   floral organs (Favaro et al., 2003). SVP-group MADS-box genes were first identified as
90   flowering suppressor regulators in Arabidopsis. In rice, their roles in regulating meristem identity
91   are well conserved, and their involvement in determining flowering time is not significant (Lee
92   et al., 2008).
93   To explore their role in the photoperiod insensitivity of oat, the MADS-box gene family was
94   identified at the genome-wide level. In this study, 16 MADS members were identified in *Avena*
95   *sativa*, and their phylogenetic relationship, gene structure, conserved motifs, chromosome
96   localization and collinearity were analyzed, along with *cis*-elements in the promoter region of all
97   identified MADS-box genes. Transcriptome data conducted in the initial stage of oat panicle
98   differentiation in the traditional oat HongQi2hao (HQ2) and photoperiod-insensitive oat MSY4
99   under short days were used for differential expression analysis. In addition, the expression
100   patterns of candidate genes at different panicle differentiation stages under short days were
101   analyzed. Our results help to further reveal the biological function of MADS genes in
102   photoperiod-insensitive oat and help to lay a foundation for revealing the mechanism of
103   photoperiod insensitivity in oat.
104
105   **Materials & Methods**
106   **Identification of MADS genes in *Avena sativa* L.**
107   To identify the potential MADS-box genes in oat, the genome sequences were obtained from the
108   GrainGenes database (https://wheat.pw.usda.gov/GG3/graingenes_downloads/oat-ot3098). The
109   MADS-box protein sequences of Arabidopsis (https://www.arabidopsis.org) and rice
110   (http://rapdb.dna.affrc.go.jp/download/irgsp1.html) were downloaded. Hidden Markov Model-
111   based searches (http://hmmer.janelia.org/), built from these known MADS-box protein
112   sequences, were used to search the MADS-box proteins in oat and as queries to search against
113   the oat protein databases with the BLASTP program with an e-value of $1 \times e^{-10}$ as the threshold.
114   The software pfamscan and the PFAM A database were used to annotate the domains of the
115   candidate *AsMADS* sequences, and the sequence containing the PF00319 domain was determined
116   to be the final MADS-box sequence in oat. The information of sequence length, molecular
117   weight, isoelectric points, and the instability index was obtained from the Expsay website
118   (http://web.expasy.org/protparam/) (Panu et al., 2012). The subcellular localization was predicted
119   using the Softberry website
120   (http://www.softberry.com/berry.phtml?topic=protcomppl&group=programs&subgroup=proloc).
121   **Sequence alignment and phylogenetic analysis**

122 The MADS-box protein sequences of Arabidopsis (https://www.arabidopsis.org) and rice
123 (http://rapdb.dna.affrc.go.jp/download/irgsp1.html) were downloaded and contained 108 and 75
124 sequences, respectively. Sequence alignment and evolution analysis were carried out on the
125 MADS protein sequences identified in oat, Arabidopsis and rice. Mafft
126 (https://omictools.com/mafft-tool) was used for protein multiple sequence alignment. DNAMAN
127 software was used to align sequences and recheck data result. Both NCBI batch CDD searches
128 and pfamscan were used to double check the conserved domains. TBtools software
129 (http://www.tbtools.com/) was used for visual display (Chen et al., 2020). MEGA version 7 was
130 used for neighbor-joining (NJ) tree construction based on the alignment of MADS proteins
131 (Kumar et al., 2018). AsMADS genes were classified according to their phylogenetic
132 relationships with the corresponding Arabidopsis (Parenicová et al., 2003) and rice (Arora et al.,
133 2007) MADS genes.
134 **Gene structure, conserved motif analysis, *Cis*-element and protein structure analysis**
135 Gene structure prediction was performed in GSDS (http://gsds.cbi.pku.edu.cn/). The conserved
136 motifs were analyzed by MEME software (http://meme-suite.org/) (Bailey et al., 2009).The
137 upstream regulatory regions (2 kb from the translation start site) of *AsMADS* genes were
138 obtained from the whole genome sequence of *Avena sativa* by TBtools. The *cis*-elements on the
139 promoter were predicted by the website
140 http://plantregmap.cbi.pku.edu.cn/binding_site_prediction.php. The positions of the binding sites
141 in the physical map of the gene promoters are marked and displayed. Protein secondary structure
142 was investigated by the Prabi website (https://npsa-prabi.ibcp.fr/cgi-
143 bin/npsa_automat.pl?page=npsa_sopma.html), and the 3D structure was predicted on the
144 SWISS-MODEL website (https://swissmodel.expasy.org/interactive).
145 **Chromosome localization and collinearity analysis**
146 According to the position of *AsMADS* genes on the chromosome, the website
147 http://mg2c.iask.in/mg2c_v2.0/ was used to draw the chromosome physical location map.
148 MCScanX software was used to perform family gene collinearity analysis based on chromosome
149 length information and gene structural annotation information. An intraspecific collinearity map
150 of oat and an interspecific collinearity map of oat, rice and Arabidopsis were constructed.
151 **Transcriptional profile analysis**
152 For *AsMADS* gene expression analysis, RNA-seq data of *Avena sativa* L. materials with different
153 photoperiod sensitivities under short-day conditions were obtained from previous laboratory data
154 (An et al., 2020; Becker & Theissen 2003). Short-day treatment-related transcriptome analysis
155 was conducted in the initial stage of panicle development in that study, in which 10 MADS
156 genes were differentially expressed in the panicles and leaves of HQ2 and MSY4. Heatmaps
157 were generated using these data. qPCR data results of 10 AsMADS genes was normalized by z-
158 score. Heatmap is performed in Metware cloud platform
159 tool(https://cloud.metware.cn/#/tools/tool-form?toolId=168). Each bar represents a gene. Red
160 indicates that the gene is up-regulated, and blue indicates that the gene is down-regulated. GO
161 function annotation of MADS genes (www. geneontolgy.org)..

162

Plant materials and treatments

163
Similar to the materials used in the previous transcriptome study, MSY4 and HQ2 were used for
164
specific expression analysis at different panicle developmental stages under short-days condition
165
(12 h). The seeding and shading methods were described in previous studies[1-3]. The young
166
panicles, including those at the initial stage, elongation stage, spikelet differentiation stage, floret
167
differentiation stage, pistil differentiation stage, and tetrad stage, were collected for expression
168
analysis. Collected tissues were immediately frozen in liquid nitrogen and stored at -80°C until
170
RNA isolation was performed.

171
Total RNA extraction and qRT–PCR expression analysis
172
The total RNA of oat panicles was extracted using a TransZol Up Plus RNA Kit (Transgene,
173
Beijing, China) and then reverse transcribed into cDNA by a TransScript® One-Step gDNA
174
Removal and cDNA Synthesis Kit. The integrity of the RNA was analyzed by agarose gel
175
electrophoresis, and the concentration and purity of the RNA were detected by a NanoDrop 2000.
176
The cDNA was stored at −20°C for subsequent qRT–PCR. Specific primers for candidate genes
177
in the MADS family were designed for qRT–PCR analysis using the Actin gene of oat as an
178
internal reference gene (Yang et al., 2013). qRT–PCR was performed with SYBR-Green on a
179
Jena Qtower 2.2 analyzer. According to the manufacturer's instructions, the 20 μL reaction
180
contained 1 μL cDNA, 400 nM of each primer and 10 μL SYBR Green Mix. The amplification
181
conditions were 95°C for 1 min and 40 cycles of 95°C for 10 s, 60°C for 10 s and 72°C for 10 s,
182
with a melting curve over a temperature range of 60-95°C. Each experiment used three
183
biological replicates and three technical replicates. The relative expression levels of genes were
184
calculated using the $2^{-\triangle\triangle Ct}$ method (Schmittgen 2008). Gene-specific DNA primers for qPCR
185
are listed in supplementary file 7.

186

187
Results
188
Identification and characterization of the MADS-box gene family in *Avena sativa* L.
189
Based on the oat genome (OT3098), a total of 16 MADS-box genes with the PF00319 domain
190
were identified through Hidden Markov Model, Blastp search and Pfam annotation, which were
191
named *AsMADS1* to *AsMADS16*. Their basic properties were systematically evaluated, including
192
gene ID and location, protein size, number of exons and introns, molecular weight, isoelectric
193
points, instability index, GRAVY, and subcellular location (Table 1). The protein length of the
194
AsMADS genes ranged from 142 to 278 amino acids, with 1 to 10 exons. The protein molecular
195
weight ranged from 16.11 kDa (*AsMADS11*) to 31.61 kDa (*AsMADS2*), and the isoelectric points
196
varied from 5.52 (*AsMADS3*) to 9.28 (*AsMADS16*). The hydrophobicity of the 16 proteins was
197
negative. The instability index ranged from 44.82 to 65.59. The subcellular location prediction
198
indicated that all members were located in the nucleus. The above results indicated that *AsMADS*
199
genes were unstable hydrophobic nucleoproteins.
200
Multiple sequence alignment and phylogenetic relationship analysis of MADS-box genes in
201
***Avena sativa* L.**

202 A multiple sequence alignment analysis of the 16 AsMADS proteins was conducted using mafft.
203 The N-terminus of the sequence was conserved (Supplementary File 1). The 16 AsMADS
204 protein sequences were analyzed for the presence of MADS-box and other domains using an
205 NCBI batch CDD search. Our results showed that all the AsMADS proteins contained the M
206 domain, and 13 out of 16 AsMADS proteins contained the K domain, except for AsMADS4,
207 AsMADS9, and AsMADS11 (Fig. 1). Moreover, 14 out of the 16 members belonged to type II
208 MADS, and the remaining two (AsMADS9 and AsMADS11) belonged to type I MADS (Fig. 1,
209 Supplementary File 2 and 3).
210 To evaluate the evolutionary relationships among the AsMADS proteins, a phylogenetic tree was
211 constructed using a bootstrapped neighbor-joining (NJ) method with the amino acid sequences of
212 207 MADS genes (16 from oat, 108 from Arabidopsis, and 83 from rice). The phylogenetic
213 analysis indicated that the 16 AsMADS members were grouped into 9 subfamilies: SEP/AGL2,
214 AGL6, SQUA, AGL12, AG, BS, SVP, Mα, and MIKC* (Fig. 2). No members were grouped into
215 the TM3/SOC1, AGL17, AGL15, FLC or Mγ subfamilies. The results showed that the SVP
216 subfamily contained 3 AsMADS members, the SEP/AGL2, SQUA, AG, BS and Mα subfamilies
217 contained two members, and the remaining three subfamilies contained only one gene (Fig. 2,
218 Supplementary File 3). In short, MADS genes in oats consisted of type I genes (*AsMADS9* and
219 *AsMADS11*), MIKC* (*AsMADS4*), and MIKC^c-type genes (13 other AsMADS members).
220 **Structural analysis and conserved motif composition of the *AsMADS* gene family**
221 Gene structure prediction was performed in GSDS website, which showed that 15 *AsMADS*
222 members contained multiple introns and exons, with the number of exons ranging from 5 to 10
223 and the number of introns ranging from 4 to 9; *AsMADS9* only contained one exon (Table 1, Fig.
224 3c). *AsMADS3, AsMADS8,* and *AsMADS13,* which were grouped in the SVP subfamily, had a
225 similar intron/exon pattern, but *AsMADS9* and *AsMADS11* had radically different structures,
226 even though they were grouped in the same subfamily.
227 The secondary structure of AsMADS proteins comprised an alpha helix, extended strand, beta
228 turn, and random coil. The AsMADS proteins had a large proportion of alpha helix amino acids
229 (>47%), followed by random coils (Supplementary File 4). Except for AsMADS11, 15 of the 16
230 AsMADS proteins had similar 3D structures (Fig. 4), indicating similar functions. Compared
231 with other genes, it is clear that the 3D predicted structure of AsMADS11 contains less α-helices
232 and more β-sheets. This makes the 3D predicted structure of AsMADS11 look simpler.
233 However, the secondary structural pattern of AsMADS11 was similar to that of the other
234 members (Supplementary File 4).
235 The full-length protein sequences of 16 AsMADS were used to investigate the conserved motifs.
236 In total, 15 different motifs were identified, and motifs 1, 2, 3 and 5 were widely distributed,
237 indicating that they might be more conserved. Interestingly, motif 11 only existed in the BS
238 subfamily (*AsMADS7* and *AsMADS15*), which may be related to its evolutionary history (Fig. 3b,
239 Supplementary File 3).
240 **Chromosome localization and collinearity analysis of *AsMADS* genes**

241 Chromosomal distribution of the *AsMADS* gene family was visualized using TBtools and the oat
242 genome annotation information. The 16 *AsMADS* genes were located on chromosomes 1D, 2D,
243 3D, 4D, 6D, 7D, 1A, 3A, 6A, 7A, 2C and 6C (Table 1). Briefly, chromosomes 1D, 2C, 3A, and
244 4D harbored 2 *AsMADS* genes, whereas the other chromosomes possessed only one *AsMADS*
245 gene. Additionally, most members were located on the ends of the chromosome, except for
246 *AsMADS8* and *AsMADS10* (Fig. 5a).
247 The intraspecific and interspecific collinearity of MADS-box genes was visualized using
248 TBTools. There was no collinearity among the 16 *AsMADS* genes on the oat chromosomes. The
249 interspecific collinearity analysis among Arabidopsis, rice and oat showed that there were 16
250 pairs of collinear genes between oat and rice, and one gene was syntenic among oat (*AsMADS2*),
251 rice (*Os01g10504.1*) and Arabidopsis (*AT4G18960*), which was annotated as AG (Fig. 5b). The
252 results showed that there was a high degree of conservation and consistency in the linear
253 relationship of MADS-box gene evolution between oat and rice.
254 **Prediction of *cis*-elements in the promoters of *AsMADS* genes**
255 The 2 kb upstream region of the *AsMADS* genes was extracted by TBtools, and submitted to the
256 online website plantregmap to search for *cis*-elements. The top 12 putative *cis*-elements in the
257 *AsMADS* promoters are shown (Fig. 6). In addition to typical promoter elements, such as TATA
258 boxes and CAAT boxes, G-box, circadian, MYB, MYC, STRE, ABRE, as-1, CGTCA-motif and
259 TGCAG-motif elements were predicted. The promoters of five *AsMADS* members contained
260 circadian elements, namely, *AsMADS1*, *AsMADS7*, *AsMADS8*, *AsMADS11* and *AsMADS15*.
261 Fourteen of the 16 members contained the light-responsive element G-box, except *AsMADS9*
262 and *AsMADS15*, but *AsMADS*9 contained other light-responsive elements, such as the I-box and
263 sp1 (Supplementary File 5). These results indicated that the promoters of all *AsMADS* members
264 contained light-responsive *cis*-acting elements.
265 **GO enrichment and transcriptome expression analysis of *AsMADS* genes**
266 For the GO classification, the 16 *AsMADS* genes were categorized into three main categories:
267 biological processes, cellular components and molecular functions (Fig. 7). *AsMADS* genes
268 categorized as flower development (GO:0009908), floral meristem determinacy (GO:0010582),
269 floral whorl structural organization (GO:0048459), floral organ formation (GO:0048449), and
270 rhythmic process may be related to the photoperiod insensitivity of oat (Supplementary File 6).
271 Based on previous transcriptome data from oat, a heatmap of the *AsMADS* gene expression
272 levels at the initial stage of oat panicle differentiation in HQ2 and MSY4 under short days was
273 drawn. Ten of 16 *AsMADS* members were differentially expressed in the transcriptome data. No
274 matter in panicles or leaves, *AsMADS2*, *AsMADS11*, and *AsMADS16* were upregulated in MSY4,
275 and *AsMADS3* and *AsMADS12* were downregulated in MSY4 (Fig. 8).
276 **Expression analysis of *AsMADS* genes in HQ2 and MSY4 under short-day conditions**
277 In order to explore the expression specificity, the expression of *AsMADS* gene among materials
278 with different photoperiod sensitivities was carried out. In HQ2, the panicle can only develop to
279 the branch differentiation stage under short days, whereas in MSY4, it can complete the whole
280 panicle differentiation process (An et al., 2018). Gene expression data for qPCR are listed in

281 supplementary file 8. The expression levels of MSY4 and HQ2 were compared in the first three
282 panicle differentiation stages. Compared with HQ2, *AsMADS3, AsMADS8, AsMADS11,*
283 *AsMADS13,* and *AsMADS16* were upregulated at these three differentiation stages in MSY4,
284 while *AsMADS12* was downregulated. *AsMADS6* and *AsMADS9* were downregulated in the
285 initial stage and elongation stage and then upregulated in the branch differentiation stage in
286 MSY4 than in HQ2, while *AsMADS2* was downregulated in the initial stage and showed
287 increased expression in the following two stages. The *AsMADS1*5 expression level remained
288 basically unchanged throughout the panicle differentiation process between MSY4 and HQ2.
289 With the development of the panicle in HQ2, the expression levels of the *AsMADS3, AsMADS8,*
290 *AsMADS12* and *AsMADS13* genes gradually decreased (Fig. 9).
291 In order to study the expression profile of *AsMADS* genes in MSY4 under short-day conditions
292 during the entire panicle differentiation stages, real-time fluorescence quantitative analysis was
293 carried out. With the development of the panicle in MSY4, the expression levels of the
294 *AsMADS9* and *AsMADS11* genes gradually decreased. The expression levels of *AsMADS15* and
295 *AsMADS16* were basically unchanged. The expression levels of the other six members fluctuated
296 at different stages of panicle differentiation (Fig. 10).
297
298

299 **Discussion**
300 Oat is a long-day crop, which limits the expansion of its growing area. Using traditional breeding
301 methods to change the photoperiod sensitivity of oats makes it possible to expand the oat
302 planting area, accelerate the breeding rate, and increase the yield of oats. To date, photoperiod-
303 insensitive oats have been created, but the underlying mechanism is unclear. Based on a previous
304 transcriptome study (An et al., 2020), many candidate genes were found, so we focused on
305 *MADS* genes due to their function in flower development and expression differences in
306 transcriptome data.
307 The release of oat genome data allowed us to identify the MADS family at the genome level.
308 Sixteen members were identified (Table 1) and classified into 9 subfamilies (Fig. 2), including
309 the A-type, C/D-type and E-type genes in the ABCDE model. AP1/SQUA-like (A-type) genes
310 can promote the formation of floral meristems (Ferrándiz et al., 2000). *OsMADS14* and
311 *OsMADS18* are AP1/SQUA-like genes in rice. Overexpression of *OsMADS14* can shorten the
312 heading period of rice and affect the formation of floral meristems, and overexpression of
313 *OsMADS18* can cause early flowering (Jeon et al., 2000). The E-type usually forms MADS-box
314 protein complexes with A-, B-, C- and D-type proteins to work together to affect floral organ
315 morphology (Favaro et al., 2003). A total of 4 E genes (*SEP1/2/3/4*) were identified in
316 Arabidopsis, and 5 SEP genes, namely, *OsMADS1, OsMADS5, OsMADS24, OsMADS34* and
317 *OsMADS45,* were identified in rice (Pelucchi et al., 2002). *OsMADS1* is the most detailed SEP-
318 like gene, and it plays a key role in the morphogenesis of floral organs (Prasad et al., 2001). The
319 SVP gene controls flowering time in most dicot plants and is an inhibitor of flowering
320 (Hartmann et al., 2000). However, the expression levels of *AsMADS8* and *AsMADS9* in the first

321   seven stages of panicle development were also significantly higher than those of other *AsMADS*
322   genes (Fig. 10). All of results indicated that SVP genes promoted the process of panicle
323   development in MSY4 under short-day conditions.
324   Among relative species of oat, the numbers of *MADS* gene family members in wheat, barley,
325   foxtail millet, maize and brachypodium were 300 (Raza et al., 2021), 34 (Kuijer et al., 2021), 89
326   (Lai et al., 2022), 211 (Zhao et al., 2021) and 57 (Wei et al., 2014), respectively. The expansion
327   and contraction of gene families is the result of the interaction between the plant and the external
328   environment. The reason why the number of MADS genes in oats is less than that in other
329   species may be the result of selection of this gene family during the evolution of oats, or the
330   phenomenon of expansion in other species. The specific reasons need to be further studied.
331   Plant MADS proteins were conserved (Favaro et al., 2002; Kuijer et al., 2021; Zobell et al.,
332   2010), and MADS proteins of oat were also conserved according to the intron/exon pattern,
333   motif components and predicted 3D structures (Fig. 3-4). *AsMADS9* and *AsMADS11* are type I
334   MADS genes, and their gene structures are completely different. *AsMADS9* contains only 1 exon
335   and no introns, while *AsMADS9* has 5 exons and a very long intron (Table 1, Fig. 3). Analysis of
336   *cis*-elements revealed that all *AsMADS* genes contained light-responsive elements (Fig. 6).
337   Therefore, the expression of *AsMADS* genes may be activated or inhibited by short-day
338   conditions during panicle development in oats. Non-vernalized spring wheat grown under a
339   short-day photoperiod accumulates *VEGETATIVE TO REPRODUCTIVE TRANSITION 2*
340   (*TaVRT2*) and shows a delay in flowering, suggesting that *TaVRT2* is regulated independently by
341   photoperiod (Kane et al., 2007). *GmAGL1* was much more effective at promoting flowering
342   under long-day conditions than under short-day conditions and *GmAGL1* overexpression not
343   only resulted in early maturation but also promoted flowering and affected petal development
344   (Zeng et al., 2018). We found that the expression levels of the *AsMADS3*, *AsMADS12*, and
345   *AsMADS13* genes gradually decreased with the development of the panicle in HQ2, and the
346   expression levels of *AsMADS3*, *AsMADS11* and *AsMADS13* were higher in MSY4 than in HQ2
347   (Fig 9). The expression levels of *AsMADS6, AsMADS8, AsMADS12,* and *AsMADS13* fluctuated
348   with panicle development (Fig 10). *AsMADS2*, *AsMADS8*, *AsMADS12* and *AsMADS16* belonged
349   to the AG, SVP and SQUA subfamilies (Supplementary File 3). The main genes that promote
350   MSY4 panicle development under short-day conditions may be SVP, SQUA and Mα genes. In
351   short, high expression of *AsMADS* genes in MSY4 promoted panicle development, while low
352   expression in HQ2 resulted in the arrest of panicle development.
353   Combined with previous transcriptome studies, the photoperiod pathway of MSY4 in response to
354   short days was predicted. After the seedlings were unearthed, the expression of photoreceptors
355   changed upon sensing inductive sunlight conditions (Takano et al., 2005). The expression of
356   *PhyB* increased, and the expression of *PhyC* and *Cry1* decreased. Photoreceptors transmit light
357   signals to circadian genes. The expression levels of *CCA1* and *PRR* genes both decreased. The
358   expression of *GI* decreased, as it is regulated by the circadian clock and can affect the magnitude
359   of circadian rhythm changes. The expression of *CO* in the phloem activates the flower-flowering
360   pathway integration gene *FT* and initiates plant flowering. However, *FT* was not differentially

361 expressed in the initial stage. The factor that actually causes MSY4 to flower under short-day
362 conditions may lie in the process of floral meristem determination. The FT protein is transported
363 from the leaf to the apical meristem cytoplasm to interact with the 14-3-3 protein and then enters
364 the nucleus together with the transcription factor FD protein to form the florigen activation
365 complex and activate the downstream floral meristem genes (Taoka et al., 2011). The MADS-
366 box plays an important regulatory role in the developmental process of determining the
367 characteristics of floral meristems. In this study, multiple MADS-box genes were detected to be
368 highly expressed in the panicles of MSY4. In particular, the high expression of the MADS-box
369 genes in the SVP, SQUA and Mα subfamilies regulate the heading and flowering of MSY4
370 under short-day conditions (Fig. 11).
371

Conclusions

373 In this study, 16 *AsMADS* genes were identified from the oat genome and could be divided into 9
374 subfamilies. The structures of *AsMADS* members were relatively conserved, but there was no
375 collinearity among them. All members contained light-responsive elements and their expression
376 levels were regulated by light. The expression profiles indicated that *AsMADS* genes belonging
377 to the SVP, SQUA and Mα subfamilies mainly regulate the panicle differentiation process of
378 MSY4 under short-day conditions. Our results can be used for the further functional analysis of
379 these *AsMADS* genes in the photoperiod response under short days.
380

Acknowledgments

382 We thank the China National Germplasm Bank for providing the photoperiod-insensitive
383 material MSY4.

384

385

References

387 Jianghong An, Rong Xiaoping, Yang Xiaohong, Li Tianliang, Zhang Ruixia, Han Bing, and Yang
388   Cai. 2018. Response of new oat germplasm to different lengths of sunlight hours.
389   *JOURNAL OF NORTHERN AGRICULTURE* 46:1-8. DOI: 10.3969/j.issn.2096-
390   1197.2018.06.01
391 Jianghong An, Yu Dongyang, Yang Xiaohong, Rong Xiaoping, Han Bing, Yang Cai, Yang Yan,
392   Zhou Haitao, and Li Tianliang. 2020. Combined transcriptome sequencing reveals the
393   photoperiod insensitivity mechanism of oats. *Plant Physiology and Biochemistry*
394   146:133-142. DOI: 10.1016/j.plaphy.2019.11.015
395 Rita Arora, Agarwal Pinky, Ray Swatismita, Singh Ashok Kumar, Singh Vijay Pal, Tyagi
396   Akhilesh K, and Kapoor Sanjay. 2007. MADS-box gene family in rice: genome-wide
397   identification, organization and expression profiling during reproductive development and
398   stress. *Bmc Genomics* 8:242. DOI: 10.1186/1471-2164-8-242
399 Timothy L Bailey, Mikael Boden, Buske Fabian A, Martin Frith, Grant Charles E, Luca Clementi,
400   Jingyuan Ren, Li Wilfred W, and Noble William S. 2009. MEME SUITE: tools for motif
401   discovery and searching. *Nucleic Acids Research* 37:W202-208. DOI:
402   10.1093/nar/gkp335

403 Annette Becker, and Theissen Günter. 2003. The major clades of MADS-box genes and their
404   role in the development and evolution of flowering plants. *Molecular Phylogenetics and*
405   *Evolution* 29:464-489. DOI: 10.1016/S1055-7903(03)00207-0
406 C. Chen, Chen H., Zhang Y, Thomas H. R., and Xia R. 2020. TBtools: An Integrative Toolkit
407   Developed for Interactive Analyses of Big Biological Data. *Molecular Plant* 13:1194-
408   1202. DOI: 10.1016/j.molp.2020.06.009
409 R Favaro, Immink RG, Ferioli V, Bernasconi B, Byzova M, Angenent GC, Kater M, and Colombo
410   L. 2002. Ovule-specific MADS-box proteins have conserved protein-protein interactions
411   in monocot and dicot plants. *Molecular Genetics and Genomics* 268:152-159.
412   10.1007/s00438-002-0746-6
413 Rebecca Favaro, Pinyopich Anusak, Battaglia Raffaella, Kooiker Maarten, Borghi Lorenzo, Ditta
414   Gary, Yanofsky Martin F., Kater Martin M., and Colombo Lucia. 2003. MADS-Box
415   Protein Complexes Control Carpel and Ovule Development in Arabidopsis. *Plant Cell*
416   15:2603-2611. DOI: 10.1105/tpc.015123
417 C Ferrándiz, Gu Q., Martienssen R., and Yanofsky M. F. 2000. Redundant regulation of
418   meristem identity and plant architecture by FRUITFULL, APETALA1 and
419   CAULIFLOWER. *Development* 127:725-734. DOI: 10.1007/PL00008234
420 U. Hartmann, Hhmann S., Nettesheim K., Wisman E., Saedler H., and Huijser P. 2000.
421   Molecular cloning of SVP: a negative regulator of the floral transition in Arabidopsis. *The*
422   *Plant journal: for cell and molecular biology* 21:351-360. DOI: 10.1046/j.1365-
423   313x.2000.00682.x
424 Katrin Henschel, Kofuji Rumiko, Hasebe Mitsuyasu, Saedler Heinz, Münster Thomas, and
425   Theißen Günter. 2002. Two Ancient Classes of MIKC-type MADS-box Genes are
426   Present in the Moss Physcomitrella patens. *Molecular Biology and Evolution* 19:801-
427   814. 10.1093/oxfordjournals.molbev.a004137 %J Molecular Biology and Evolution
428 J. S. Jeon, Lee S., Jung K. H., Yang W. S., Yi G. H., Oh B. G., and An G. 2000. Production of
429   transgenic rice plants showing reduced heading date and plant height by ectopic
430   expression of rice MADS-box genes. *Molecular Breeding* 6:581-592. DOI:
431   10.1023/A:1011388620872
432 Winter Kai-Uwe, Christof W., Kerstin K., Arend B., Charlotte K., Akira K., Heinz S., Günter T,
433   and Evolution. 2002. Evolution of class B floral homeotic proteins: obligate
434   heterodimerization originated from homodimerization. *Molecular Biology and*
435   *Evolution*:587-596. DOI: 10.1097/00004872-200018030-00002
436 NA Kane, Agharbaoui Z, Diallo AO, Adam H, Tominaga Y, Ouellet F, and F Sarhan. 2007.
437   TaVRT2 represses transcription of the wheat vernalization gene TaVRN1. *The Plant*
438   *journal : for cell molecular biology* 51:670-680. 10.1111/j.1365-313X.2007.03172.x
439 S. A. Kempin, Savidge B., and Yanofsky M. F. 1995. Molecular basis of the cauliflower
440   phenotype in Arabidopsis. *Science* 267:522-525. DOI: 10.1126/science.7824951
441 HNJ Kuijer, Shirley NJ, Khor SF, Shi J, Schwerdt J, Zhang D, Li G, and Burton RA. 2021.
442   Transcript Profiling of MIKCc MADS-Box Genes Reveals Conserved and Novel Roles in
443   Barley Inflorescence Development. *Frontiers in Plant Science* 12:705286.
444   10.3389/fpls.2021.705286
445 Sudhir Kumar, Stecher Glen, Li Michael, Knyaz Christina, and Tamura Koichiro. 2018. MEGA X:
446   Molecular Evolutionary Genetics Analysis across computing platforms. *Molecular*
447   *Biology Evolution* 35:1547-1549. DOI: 10.1093/molbev/msy096
448 D Lai, Yan J, He A, Xue G, Yang H, Feng L, Wei X, Li L, Xiang D, Ruan J, Fan Y, and Cheng J.
449   2022. Genome-wide identification, phylogenetic and expression pattern analysis of
450   MADS-box family genes in foxtail millet (Setaria italica). *Scientific reports* 12:4979.
451   10.1038/s41598-022-07103-9

452 S. Lee, Jeong D. H., and An G. 2008. A possible working mechanism for rice SVP-group
453   MADS-box proteins as negative regulators of brassinosteroid responses. *Plant signaling*
454   *& behavior* 3:471-474. DOI: 10.4161/psb.3.7.5677
455 Kwantes Michiel, Daniela Liebsch, and Wim Verelst. 2012. How MIKC* MADS-Box Genes
456   Originated and Evidence for Their Conserved Function Throughout the Evolution of
457   Vascular Plant Gametophytes. *Molecular Biology and Evolution*:293-302. DOI:
458   10.1093/molbev/msr200
459 A. Panu, Manohar J., Konstantin A., Delphine B., Gabor C., Edouard De Castro, Séverine D,
460   Volker F., Arnaud F., and Elisabeth G. 2012. ExPASy: SIB bioinformatics resource
461   portal. *Nucleic Acids Research*:W597-W603. DOI: 10.1093/nar/gks400
462 L. Parenicová, Folter S. D., Kieffer M., Horner D. S., and Colombo L. 2003. Molecular and
463   Phylogenetic Analyses of the Complete MADS-Box Transcription Factor Family in
464   Arabidopsis New Openings to the MADS World. *The Plant Cell* 15:1538-1551. DOI:
465   10.1353/hub.2002.0011
466 Nilla Pelucchi, Fornara Fabio, Favalli Cristina, Masiero Simona, Lago Clara, Pè Enrico M,
467   Colombo Lucia, and Kater Martin M. 2002. Comparative analysis of rice MADS-box
468   genes expressed during flower development. *Sexual Plant Reproduction* 15:113-122.
469   DOI: 10.1007/s00497-002-0151-7
470 K. Prasad, Sriram P., Kumar S. C., Kushalappa K., and Vijayraghavan U. 2001. Ectopic
471   expression of rice OsMADS1 reveals a role in specifying the lemma and palea, grass
472   floral organs analogous to sepals. *Development Genes Evolution* 211:281-290. DOI:
473   10.1007/s004270100153
474 Q Raza, Riaz A, Atif RM, Hussain B, Rana IA, Ali Z, Budak H, and Alaraidh IA 2021. Genome-
475   Wide Diversity of MADS-Box Genes in Bread Wheat is Associated with its Rapid Global
476   Adaptability. *Frontiers in genetics* 12:818880. 10.3389/fgene.2021.818880
477 Thomas D. Schmittgen. 2008. Analyzing Real-time PCR data by the comparative CT method.
478   *Nature Protocols* 3:1101-1108. DOI: 10.1038/nprot.2008.73>
479 S Shimada, Ogawa T, Kitagawa S, Suzuki T, Ikari C, Shitsukawa N, Abe T, Kawahigashi H,
480   Kikuchi R, and Handa H. 2009. A genetic network of flowering-time genes in wheat
481   leaves, in which an APETALA1/FRUITFULL-like gene, VRN1, is upstream of
482   FLOWERING LOCUS T. *Plant Journal* 58:668-681. DOI: 10.1111/j.1365-
483   313X.2009.03806.x
484 Cezary Smaczniak, Immink Richard G H, Angenent Gerco C, and Kaufmann Kerstin. 2012.
485   Developmental and evolutionary diversity of plant MADS-domain factors: Insights from
486   recent studies. *Development* 139:3081-3098.
487 Schilling Susanne, Alice Kennedy, Sirui Pan, S. Jermiin Lars, and Rainer Melzer. 2020.
488   Genome-wide analysis of MIKC-type MADS-box genes in wheat: pervasive duplications,
489   functional conservation and putative neofunctionalization. *New Phytologist*.
490 Makoto Takano, Inagaki Noritoshi, Xie Xianzhi, Yuzurihara Natsu, Hihara Fukiko, Ishizuka Toru,
491   Yano Masahiro, Nishimura Minoru, Miyao Akio, Hirochika Hirohiko, and Shinomura
492   Tomoko. 2005. Distinct and cooperative functions of phytochromes A, B, and C in the
493   control of deetiolation and flowering in rice. *Plant Cell* 17:3311. DOI:
494   10.1105/tpc.105.035899
495 Ken-ichiro Taoka, Ohki Izuru, Tsuji Hiroyuki, Furuita Kyoko, Hayashi Kokoro, Yanase Tomoko,
496   Yamaguchi Midori, Nakashima Chika, Purwestri Yekti Asih, Tamaki Shojiro, Ogaki Yuka,
497   Shimada Chihiro, Nakagawa Atsushi, Kojima Chojiro, and Shimamoto Ko. 2011. 14-3-3
498   proteins act as intracellular receptors for rice Hd3a florigen. *Nature Protocols* 476:332-
499   335. DOI: 10.1038/nature10272
500 Günter Theien. 2001. Development of floral organ identity: Stories from the MADS house.
501   *Current Opinion in Plant Biology* 4:75-85. DOI: 10.1016/S1369-5266(00)00139-4

502 B Wei, Zhang RZ, Guo JJ, Liu DM, Li AL, Fan RC, Mao L, and Zhang XQ. 2014. Genome-wide
503   analysis of the MADS-box gene family in Brachypodium distachyon. *Plos One* 9:e84781.
504   10.1371/journal.pone.0084781
505 Cai Yang, Zhou Haitao, Li Tianliang, Zhang Xinjun, Yang Xiaohong, Liu Wenting, and Bai Jing.
506   2014. The Breeding of Many Types of Oats Germplasm Resources Which Not Sensitive
507   to Long Photoperiod Through Interspecific Polymer Crossing. *Seed* 33:4. DOI:
508   10.16590/j.cnki.1001-4705.2014.04.062
509 T. Yang, Sun S. S., Gao S. Q., Tang Y. M., and Zhao C. P. 2013. Cloning of AsRBP1 Gene
510   from Oat(Avena sterilis) and Analysis on Its Expressions to Stresses. *Journal of Triticeae*
511   *Crops* 33:217-223.
512 Xiaohong Yang, An Jianghong, Han Bing, Zhou Hai Tao, and Yang Cai. 2018. Effect of
513   Simulated Short-day on Spike Development of Spring and Summer Sown Oat by
514   Shading. *Biotechnology Bulletin* 34:93-97. DOI: 10.13560/j.cnki.biotech.bull.1985.2017-
515   0741
516 X Zeng, Liu H, Du H, Wang S, Yang W, Chi Y, Wang J, Huang F, and Yu D. 2018. Soybean
517   MADS-box gene GmAGL1 promotes flowering via the photoperiod pathway. *Molecular*
518   *Biology and Evolution* 19:51. 10.1186/s12864-017-4402-2
519 D Zhao, Chen Z, Xu L, Zhang L, and Zou Q. 2021. Genome-Wide Analysis of the MADS-Box
520   Gene Family in Maize: Gene Structure, Evolution, and Relationships. *Genes* 12.
521   10.3390/genes12121956
522 Yang Zhao, Li Xiaoyu, Chen Wenjuan, Peng Xiaojian, Cheng Xiao, Zhu Suwen, and Cheng
523   Beijiu. 2011. Whole-genome survey and characterization of MADS-box gene family in
524   maize and sorghum. *Plant Cell Tiss Organ Cult* 105:159-173. DOI: 10.1007/s11240-010-
525   9848-8
526 Oliver Zobell, Faigl Wolfram, Saedler Heinz, Biology Thomas Münster %J Molecular, and
527   Evolution. 2010. MIKC* MADS-Box Proteins: Conserved Regulators of the Gametophytic
528   Generation of Land Plants. 27:1201-1211. 10.1093/molbev/msq005
529

Figure 1

Conserved domain structure of 16 AsMADS proteins in *Avena sativa* L.
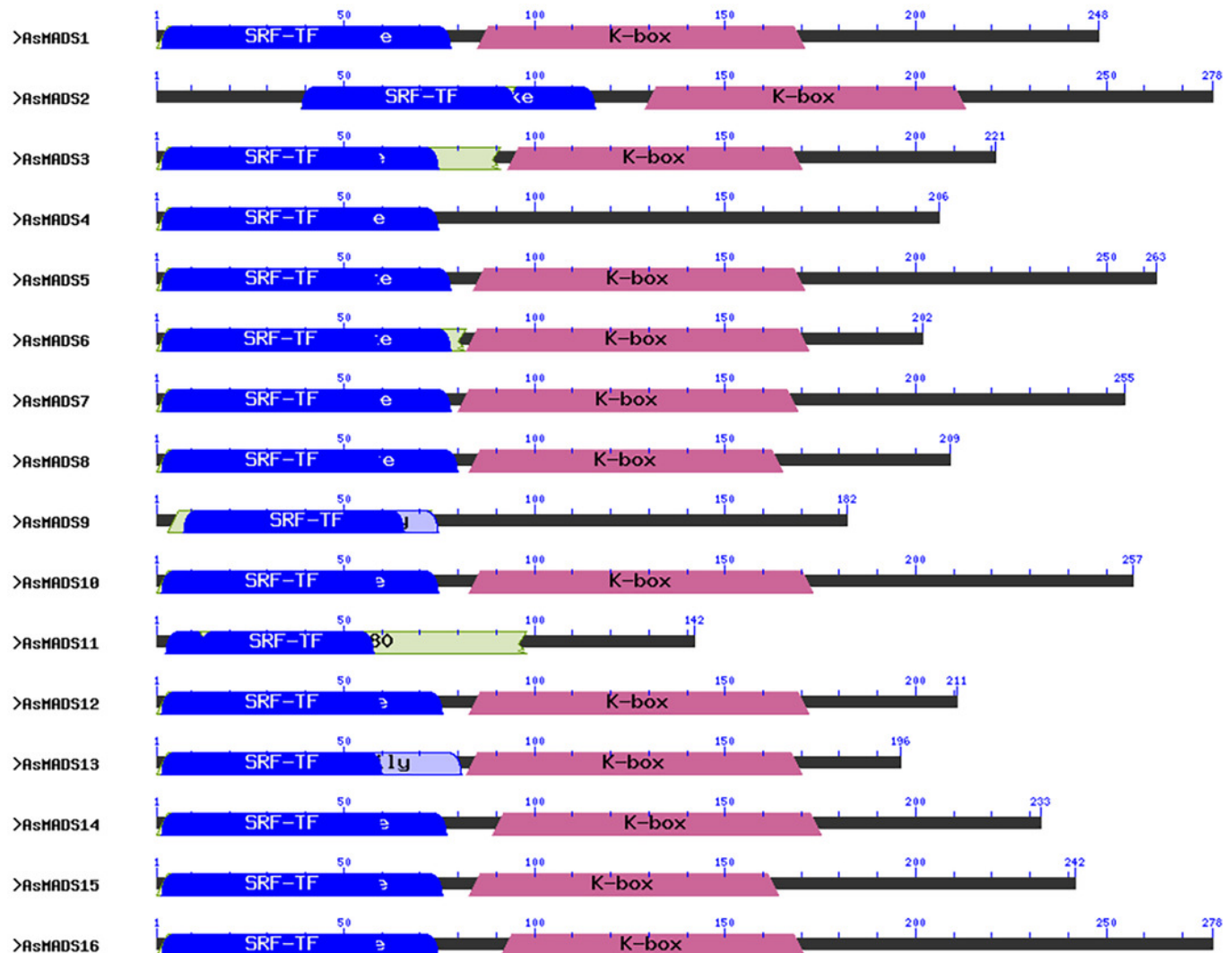
Figure 2

A phylogenetic tree of the AsMADS gene family.

The MADS proteins of oat, Arabidopsis, and rice were clustered into 14 groups. Members of different colors belong to different groups.
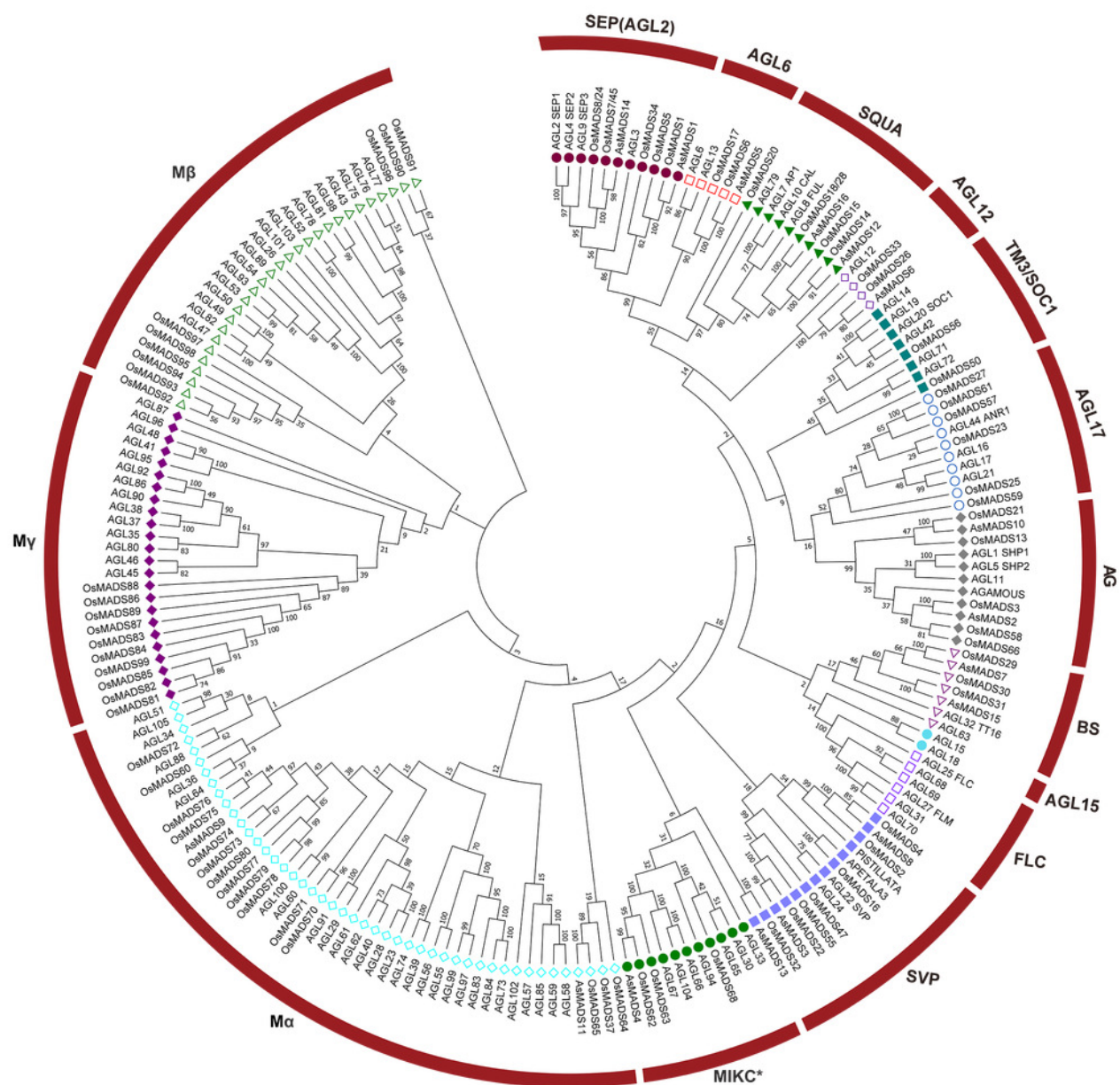
Figure 3

Gene structure and architecture of conserved protein motifs in AsMADSs.

(a) The phylogenetic tree was constructed based on the full-length sequences of oat MADS family proteins using MEGA-7 software. (b) The motif compositions of AsMADSs. Different colored boxes display different motifs. (c) The exon-intron structure of AsMADSs. Yellow lines indicate CDSs, and black lines indicate introns.
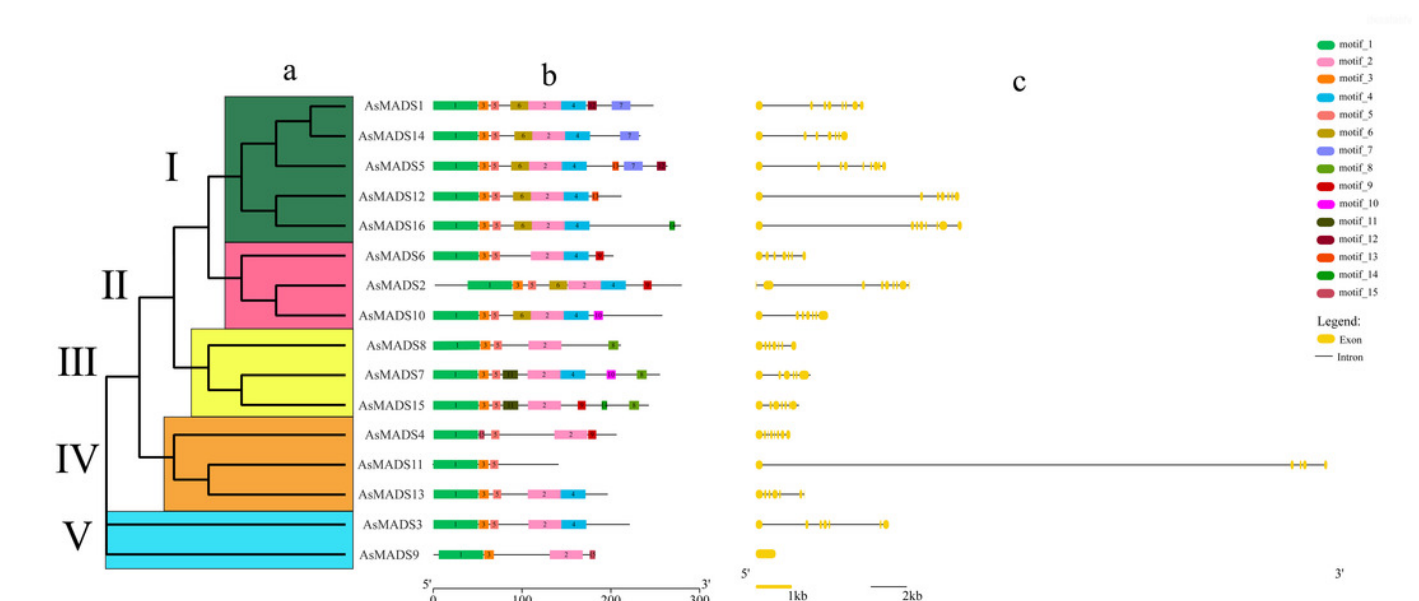
Figure 4

Predicted three-dimensional domains of 16 AsMADS proteins from oat.
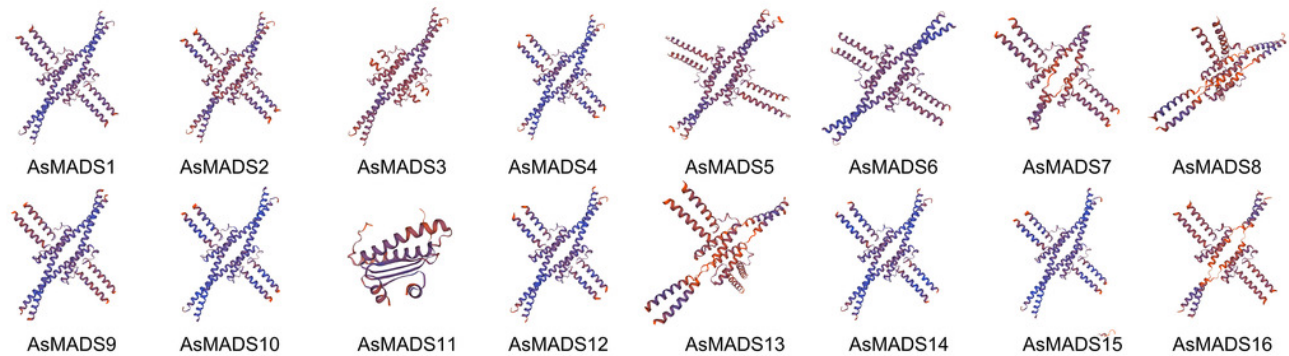
Figure 5

Chromosomal location and collinearity analysis of 16 AsMADS genes.

(a) Chromosomal location of 16 AsMADS genes in oat. (b) Collinearity analysis of AsMADSs between oat, Arabidopsis, and rice. the Os, As and At respectively indicates that *Oryza sativa*, *Avena sativa*, *Arabidopsis thaliana*.
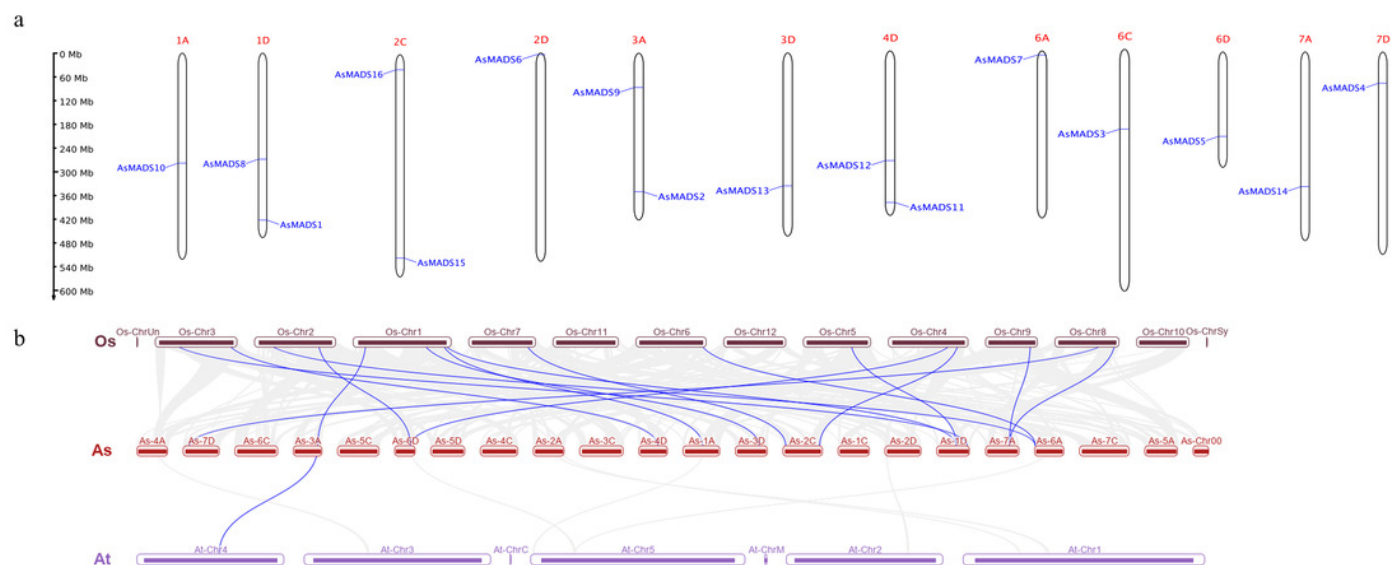
Figure 6

Prediction of *cis*-elements in the 2k upstream regulatory regions of AsMADS genes.

Different colored boxes indicate different *cis*-elements.
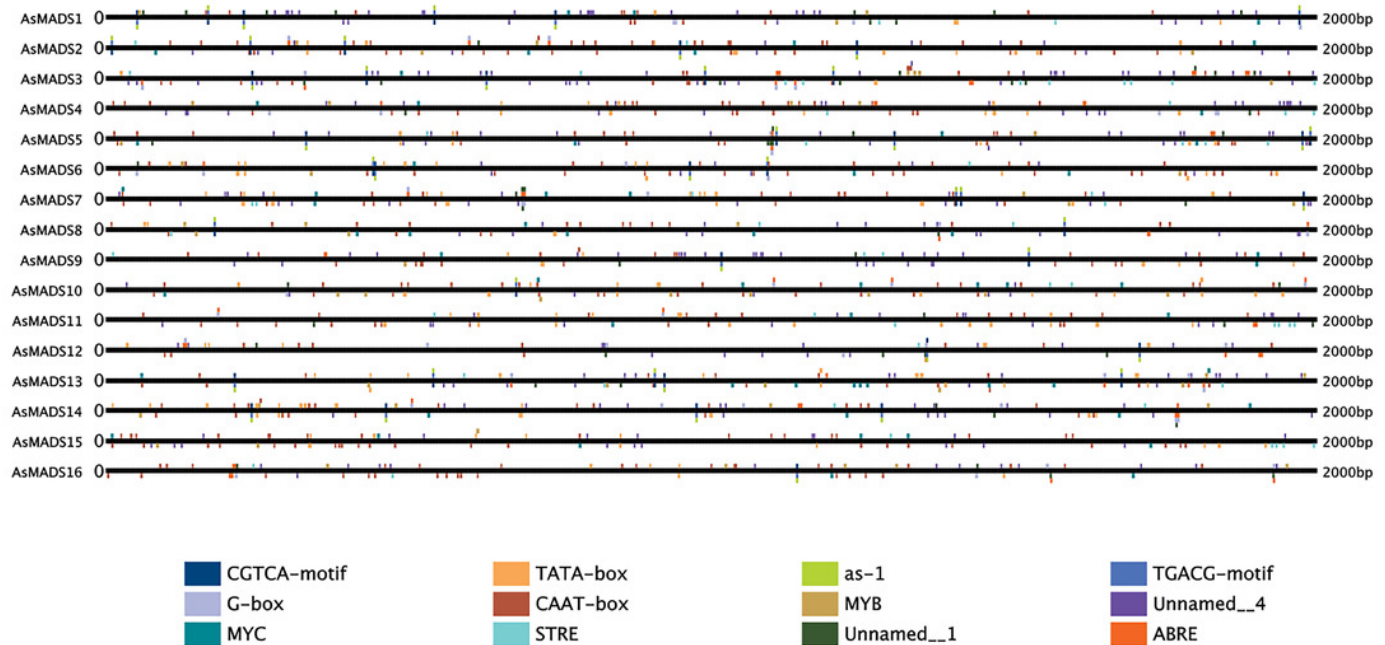
Figure 7

Gene Ontology analysis of 10 AsMADS genes from RNA-seq data.
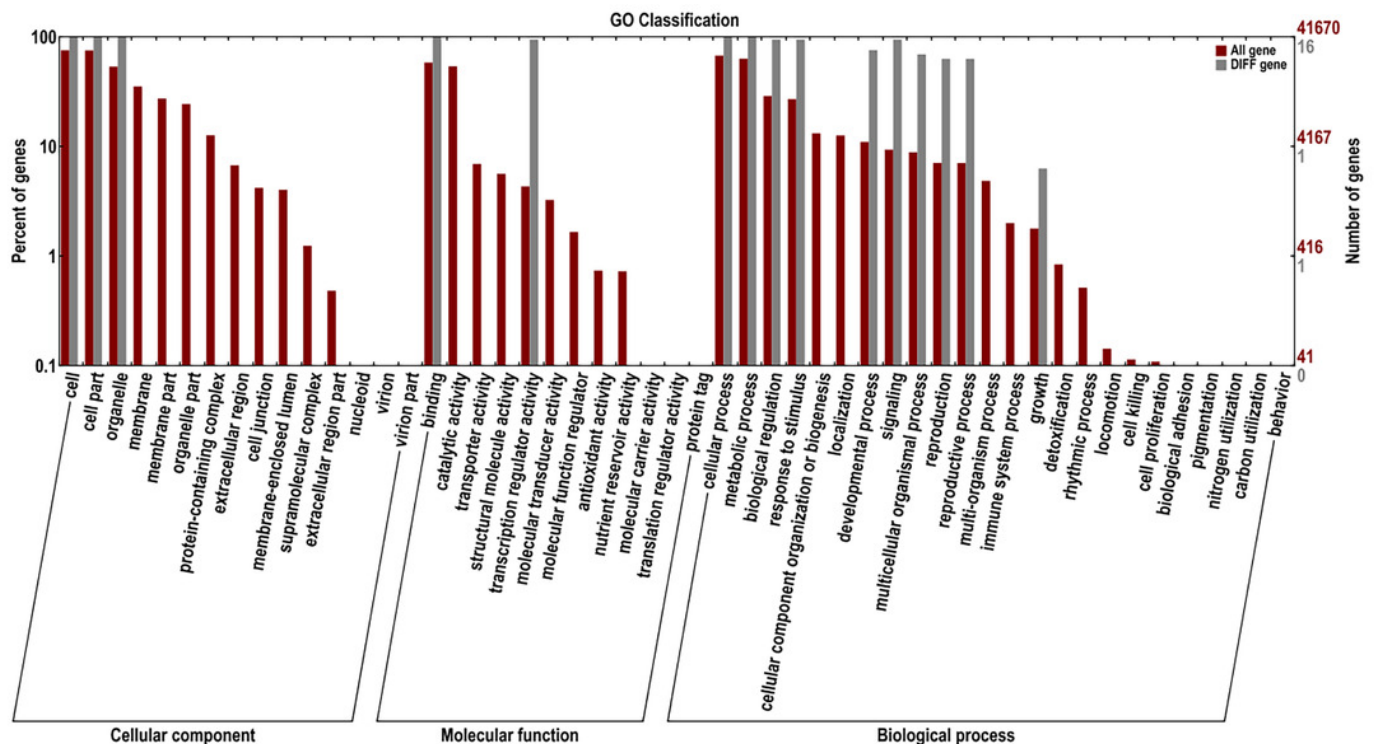
Figure 8

Expression profiles analysis of 10 AsMADS genes from RNA-seq data.

Differentially expressed genes are screened in panicles (T01, T02, T07, and T08) and leaves (T03, T04, T05, and T06) at the oat initial differentiation stage of HQ2 and MSY4 under short-day conditions.Note: T0-T04 is HQ2. T05-T08 is MSY4. T01, T02, T07, and T08 is panicle. T03, T04, T05, and T06 is leaf.
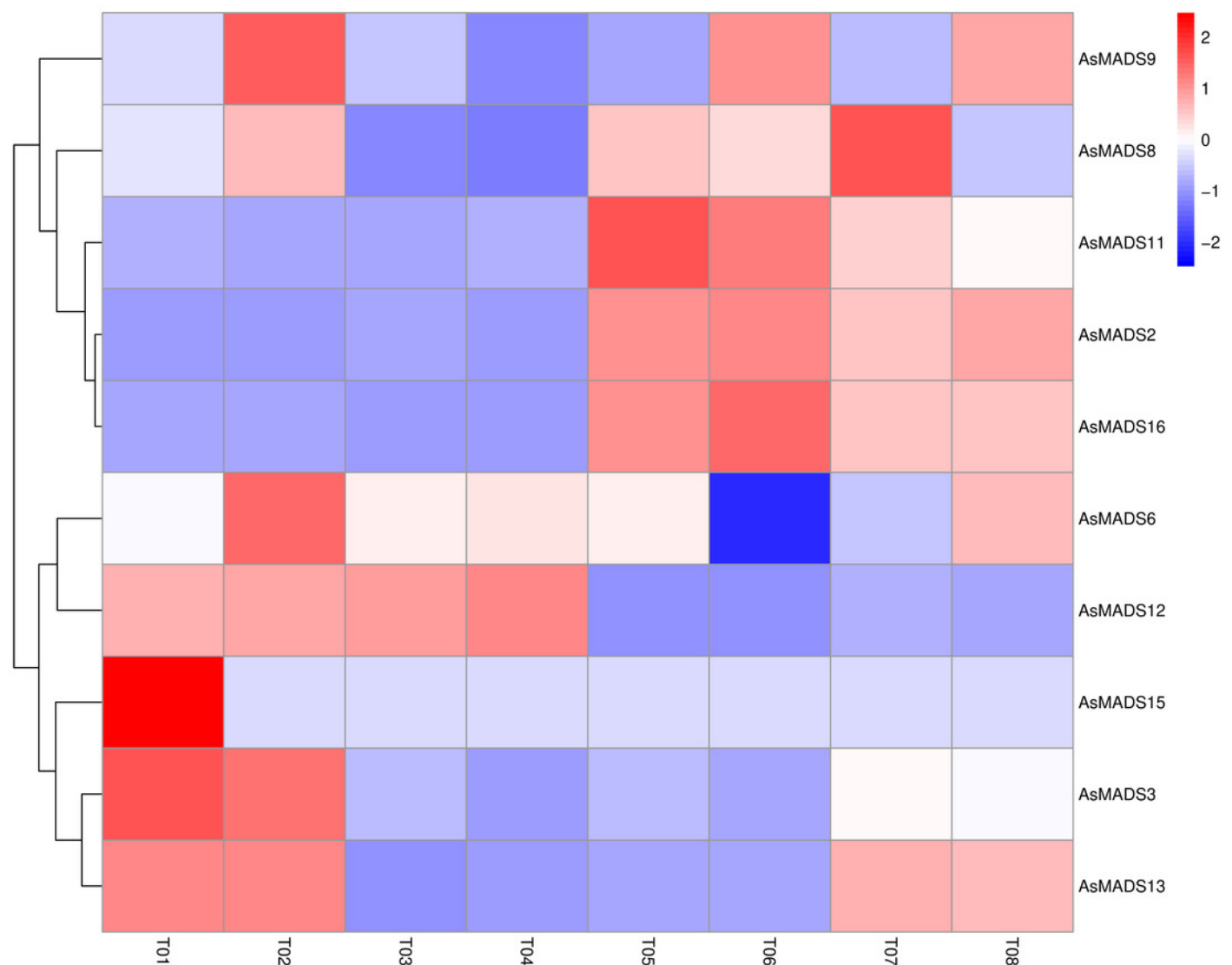
Figure 9

Gene expression of 10 AsMADS genes in the initial stage, elongation stage and branch differentiation stage of HQ2 and MSY4 under short days from qPCR.

Note: qPCR data results of 10 AsMADS genes was normalized by z-score. Heatmap is performed in Metware cloud platform tool(https://cloud.metware.cn/#/tools/tool-form?toolId=168). Each bar represents a gene. Red indicates that the gene is up-regulated, and blue indicates that the gene is down-regulated.
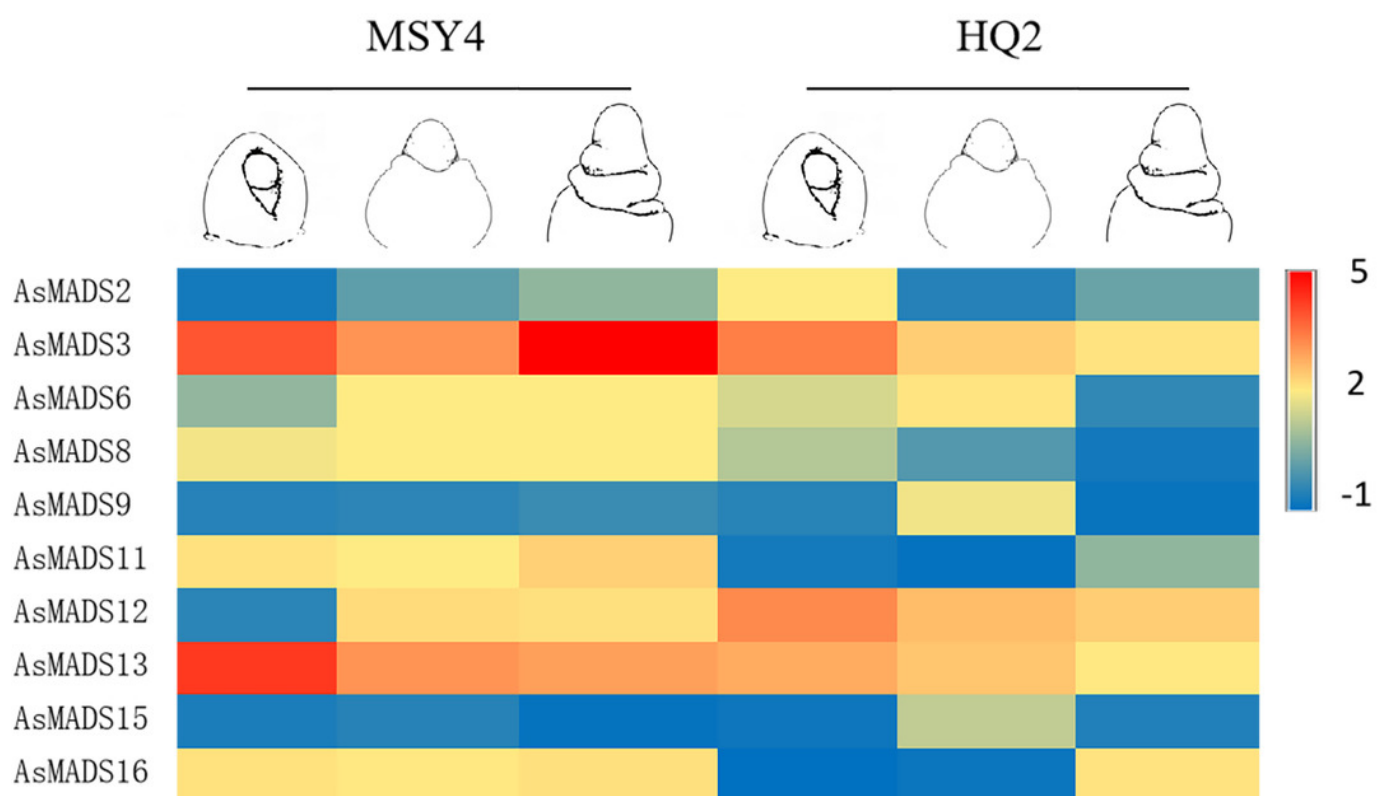
Figure 10

Expression heat map of 10 AsMADS genes at different developmental stages of MSY4 under short days from qPCR.

Note: qPCR data results of 10 AsMADS genes was normalized by z-score. Heatmap is performed in Metware cloud platform tool(https://cloud.metware.cn/#/tools/tool-form?toolId=168). Each bar represents a gene. Red indicates that the gene is up-regulated, and blue indicates that the gene is down-regulated.
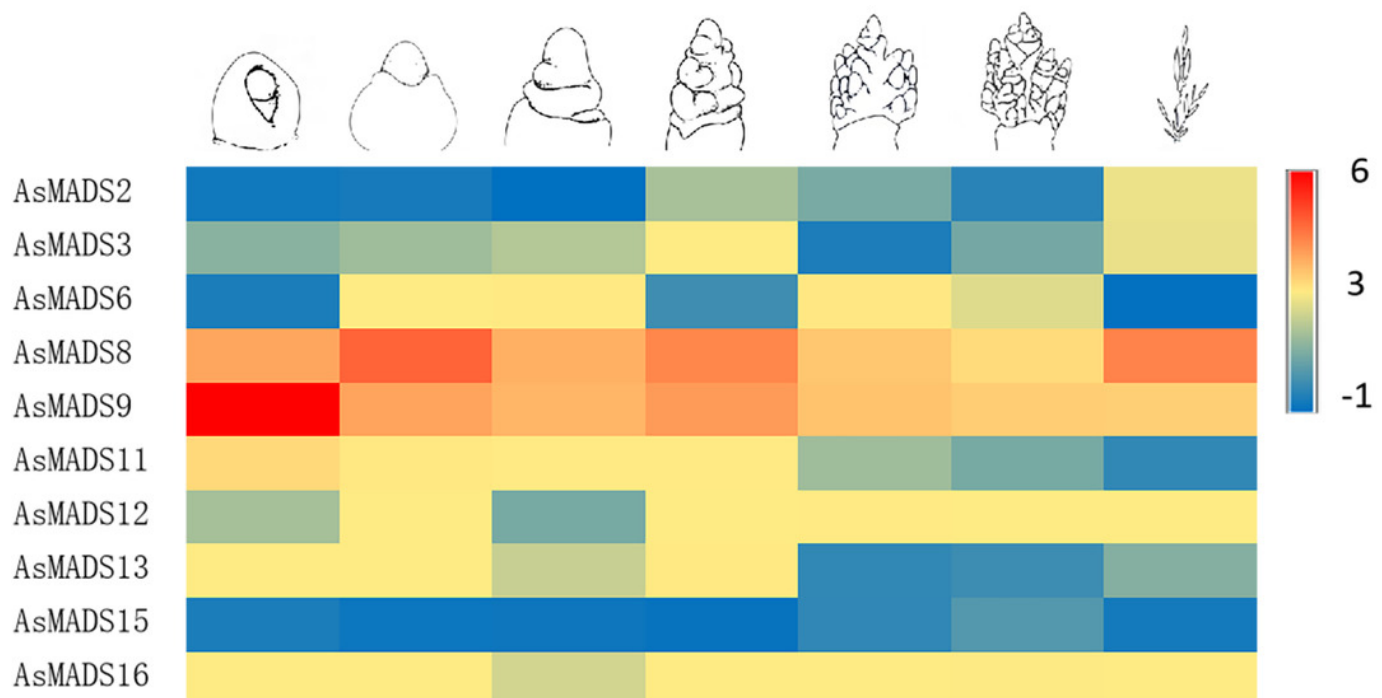
Figure 11

Predicted photoperiodic pathway of MSY4 under short-day conditions.

Red boxes indicate up-regulation, blue boxes indicate down-regulation, yellow boxes indicate inconsistent expression patterns of multiple transcripts, and green boxes indicate unchanged expression levels
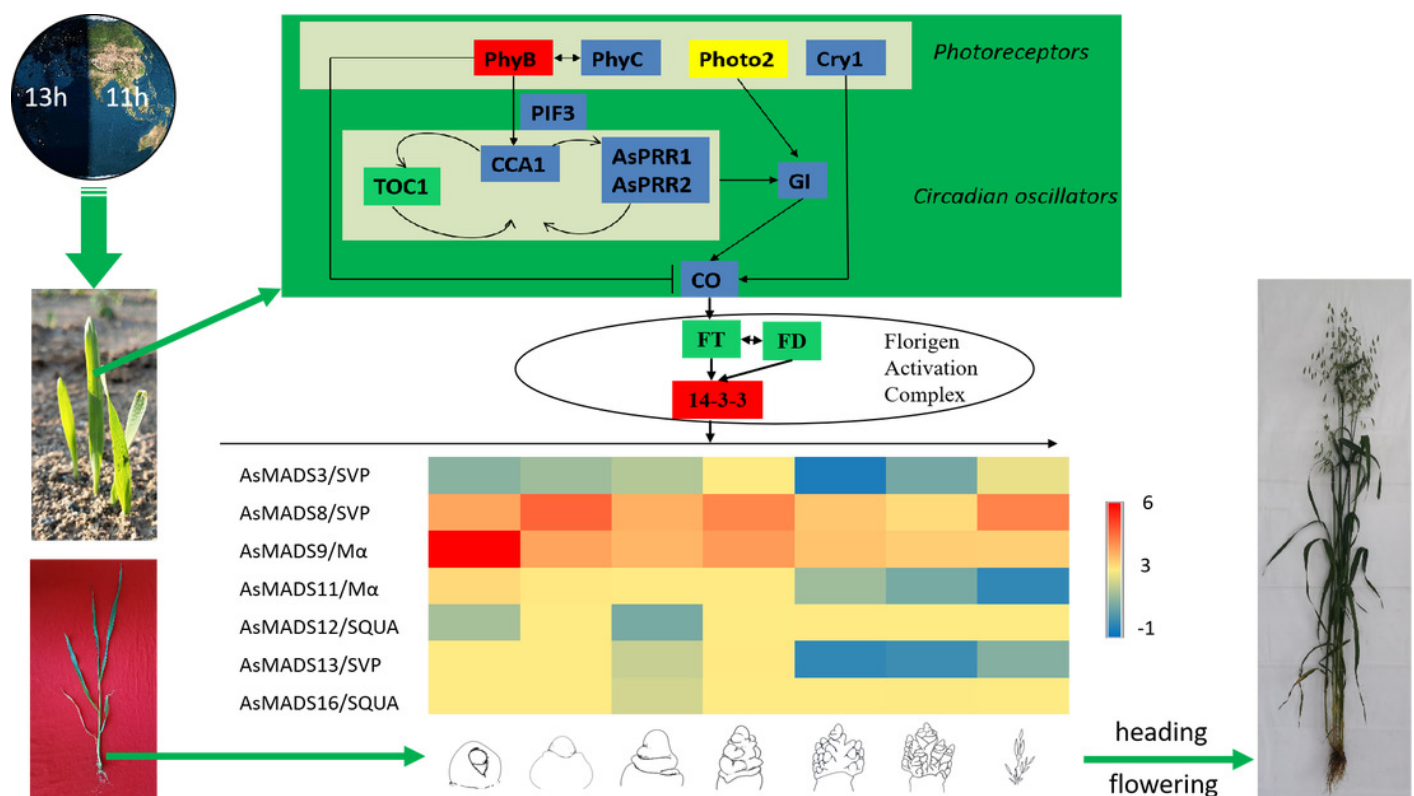
Information for the MADS gene family

1   Table 1:

2   Information for the MADS gene family

Gene Name	Gene Id	Location	Size (AA)	Exon	Intron	Molecular Weight (KDa)	Isoelectric Points	Instability Index	GRAVY	Subcellular Location
AsMADS1	TRINITY_DN13687_c0_g2_i1.mrna1	1D:440731844-440737616	248	8	7	28.33	6.46	64.41	-0.797	Nuclear
AsMADS2	TRINITY_DN231_c1_g1_i5.mrna2	3A:354464249-354472711	278	10	9	31.61	9.01	54.8	-0.839	Nuclear
AsMADS3	TRINITY_DN32614_c0_g1_i3.mrna1	6C:205578143-205585989	221	7	6	24.64	5.52	49.5	-0.634	Nuclear
AsMADS4	TRINITY_DN3261_c0_g2_i2.mrna1	7D:80735581-80737035	206	8	7	23.77	7.02	62.67	-0.492	Nuclear
AsMADS5	TRINITY_DN3337_c0_g1_i3.mrna2	6D:221314556-221321673	263	9	8	29.83	8.9	45.02	-0.776	Nuclear
AsMADS6	TRINITY_DN3733_c0_g1_i1.mrna1	2D:4056942-4066252	202	7	6	23.43	8.8	60.05	-0.553	Nuclear
AsMADS7	TRINITY_DN383_c0_g1_i1.mrna1	6A:9765559-9768798	255	7	6	28.48	6.46	61.69	-0.515	Nuclear
AsMADS8	TRINITY_DN383_c1_g1_i2.mrna1	1D:279668871-279671412	209	7	6	24.33	9.08	64.25	-0.805	Nuclear
AsMADS9	TRINITY_DN39828_c0_g6_i1.mrna1	3A:87682568-87683651	182	1	0	20.14	6.76	54.46	-0.416	Nuclear
AsMADS10	TRINITY_DN4009_c0_g1_i6.mrna1	1A:289587547-289592225	257	7	6	28.69	9.15	60.67	-0.616	Nuclear
AsMADS11	TRINITY_DN42664_c0_g1_i9.mrna1	4D:391283530-391315386	142	5	4	16.11	9.09	65.59	-0.723	Nuclear
AsMADS12	TRINITY_DN6792_c2_g1_i3.mrna1	4D:282480902-282492339	211	7	6	24.63	9.25	60.9	-0.82	Nuclear
AsMADS13	TRINITY_DN6901_c0_g1_i1.mrna1	3D:340212580-340215197	196	7	6	22.32	8.67	44.82	-0.59	Nuclear
AsMADS14	TRINITY_DN695_c0_g1_i7.mrna1	7A:351371284-351376726	233	7	6	27.03	8.96	45.71	-0.845	Nuclear
AsMADS15	TRINITY_DN9392_c0_g1_i5.mrna2	2C:535820137-535822661	242	8	7	28.18	8.52	55.2	-0.558	Nuclear
AsMADS16	TRINITY_DN9814_c0_g1_i1.mrna2	2C:39788836-39799997	278	8	7	31.51	9.28	59.65	-0.856	Nuclear